Charles University in Prague

Faculty of Mathematics and Physics

MASTER THESIS

Martin Pecka

Detection of 2D features in MARSIS ionogram pictures

Department of Software Engineering

Supervisor of the master thesis:	RNDr. Jana Štanclová, Ph.D.
Study programme:	Informatics
Specialization:	Theoretical Informatics

Prague 2013

Dedication.

I declare that I carried out this master thesis independently, and only with the cited sources, literature and other professional sources.

I understand that my work relates to the rights and obligations under the Act No. 121/2000 Coll., the Copyright Act, as amended, in particular the fact that the Charles University in Prague has the right to conclude a license agreement on the use of this work as a school work pursuant to Section 60 paragraph 1 of the Copyright Act.

In Prague date ....

Název práce: Hledání 2D jevů v ionografických snímcích přístroje MARSIS

Autor: Bc. Martin Pecka

Katedra: Katedra softwarového inženýrství

Vedoucí diplomové práce: RNDr. Jana Štanclová, Ph.D., Katedra softwarového inženýrství

Abstrakt: Práce se zabývá technikami hledání význačných prvků v ionogramech zachycených přístrojem MARSIS umístěným na kosmické sondě Mars Express. Ionogramy jsou reprezentovány jako dvourozměrné obrázky s hodnotou kódovanou pomocí barvy. Vyvíjené techniky se snaží detekovat v takových snímcích různé zajímavé křivky (definované sadou parametrů), případně měřit další parametry nalezených objektů (perioda opakování přímek).

Klíčová slova: rozpoznávání vzorů, detekce, parametrické křivky, Mars Express, vektorizace

Title: Detection of 2D features in MARSIS ionogram pictures

Author: Bc. Martin Pecka

Department: Department of Software Engineering

Supervisor: RNDr. Jana Štanclová, Ph.D., Department of Software Engineering

Abstract: The work focuses on techniques for finding significant features in ionograms captured by the MARSIS instrument onboard the Mars Express spacecraft. Ionograms are 2D images with values represented in color. The developed techniques try to detect interesting curves (parametrically defined) in such images and measure some more parameters of the found objects (like the repetition period of lines).

Keywords: pattern recognition, detection, parametric curves, Mars Express, vectorization

Contents

Introduction **2**

1 Mars Express, MARSIS and ionograms **3**

1.1 Mars Express 3

1.1.1 HRSC (*High-Resolution Stereo Camera*) 4

1.1.2 OMEGA (*Observatoire pour la Minéralogie, l'Eau, les Glaces et l'Activité*) 5

1.1.3 MARSIS (*Mars Advanced Radar for Subsurface and Ionosphere Sounding*) 6

1.1.4 PFS (*Planetary Fourier Spectrometer*) 6

1.1.5 SPICAM (*SPectroscopy for the Investigation of the Characteristics of the Atmosphere of Mars*) 7

1.1.6 ASPERA–3 (*Analyser of Space Plasmas and EneRgetic Atoms*) 7

1.1.7 MaRS (*Mars Express Orbiter Radio Science*) 8

1.1.8 Beagle 2 9

1.2 The MARSIS experiment 9

1.2.1 Subsurface sounding 10

1.2.2 Surface sounding 11

1.2.3 Ionospheric sounding 11

1.3 Ionograms 12

1.3.1 Ionospheric echo 13

1.3.2 Surface echo 13

1.3.3 Oblique ionospheric echo 14

1.3.4 Electron plasma oscillation harmonics 15

1.3.5 Electron cyclotron echoes 16

2 Title of the second chapter **18**

2.1 Title of the first subchapter of the second chapter 18

2.2 Title of the second subchapter of the second chapter 18

Conclusion **19**

Bibliography **20**

List of Tables **24**

List of Abbreviations **25**

Attachments **26**

Introduction

1. Mars Express, MARSIS and ionograms

1.1 Mars Express

First of all, let us briefly introduce the spacecraft carrying all the equipment needed to acquire ionograms. Its name is *Mars Express* (MEX) and it was launched by the *European Space Agency* (ESA) on 2 June 2003.

MEX arrived to Mars at its orbit with periapsis 250 km and apoapsis over 11,000 km on 25 December 2003 [30] with seven onboard scientific instruments and a landing module called Beagle 2. We're going to take a look at all of them in the following subsections; just Beagle 2 description is going to be rather short, because the landing sequence failed (for an unknown reason) and the lander didn't establish connection after it landed (if it landed at all)[30, p. 4].

The mission of MEX has several goals like "global studies of the surface, subsurface and atmosphere at unprecedented spatial and spectral resolutions" [30, p. viii]. One of the goals, however, stands out among all the others. It is the search for water (or its traces) on martian surface or subsurface.

Why water? There is lots of geological evidence of former water occurrence. But before the MEX mission nobody had proved or refuted presence of water on Mars in the present. Knowing more about water on Mars and its history, the scientists could postulate better hypotheses about the possibility of (former) life on the planet [30, p. ix].

The original mission lifetime of MEX was projected up to the end of 2005 (which would be 1 Martian year = 687 Earth days) [11]. However, overcoming some small problems (as the Solid State Mass Memory anomalies described in [15] or the MARSIS antennas deployment problems in 2004 [12, 13]), MEX has worked on its science goals up to this day and its science mission was extended until 2014 [17] (after 3 preceding similar extensions). Fred Jansen, MEX mission manager, said MEX had enough fuel for another 14 years of operation (at the beginning of 2012) [8]. So there is a hopeful prospect of further and even deeper Mars exploration (eg. [19] discovered an unexpected way of using the MARSIS instrument so that they "added magnetometer functionality" to MARSIS).

In the next subsections you can find out more about particular MEX instruments. The descriptions are based on [30] which you can see for more detailed information.

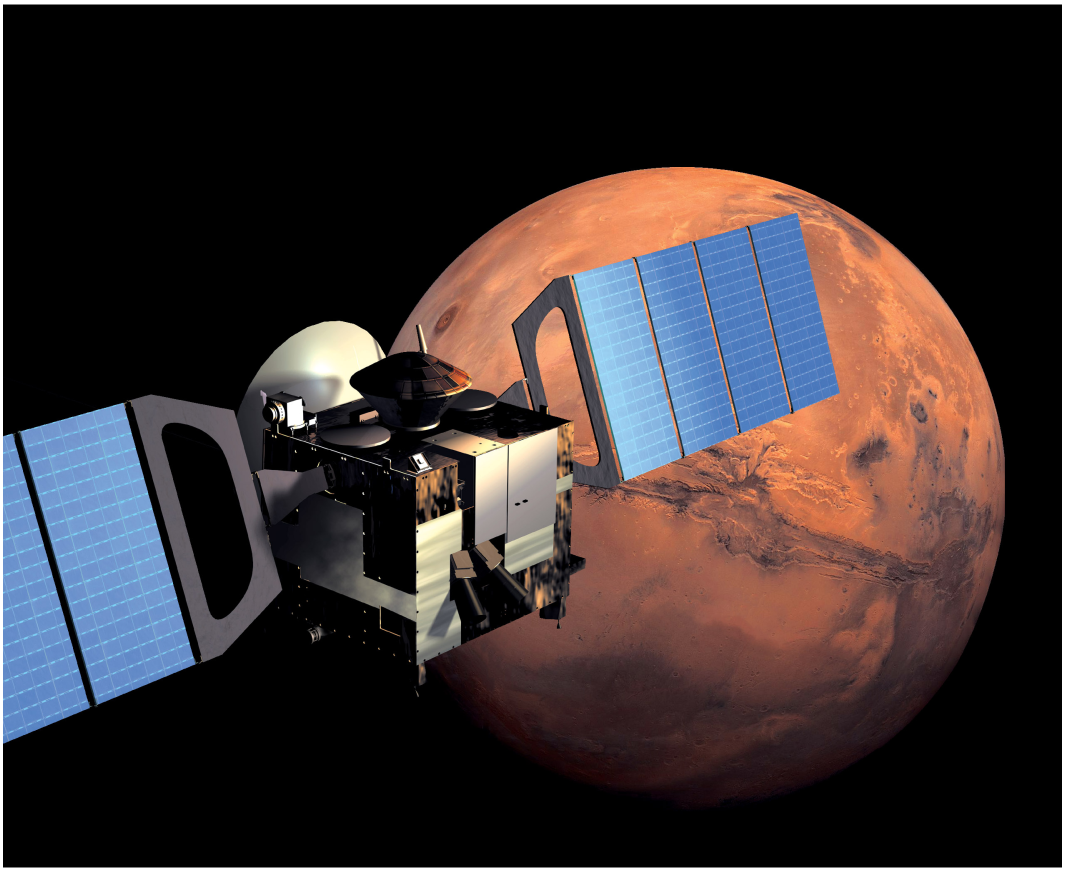

Figure 1.1: Mars Express spacecraft. Credit: ESA [14]

1.1.1 HRSC (*High-Resolution Stereo Camera*)

HRSC is a high-resolution pushbroom[1] camera for surface imaging. Its goals are to characterize surface structure and morphology at resolution 10 m.px^{-1} (regions of interest at 2 m.px^{-1}), surface topology at high vertical resolution, atmospheric phenomena, physical properties of the surface and to classify terrain and to refine the martian cartographic base. It is also intended to observe martian moons Phobos and Deimos during their approaches.

HRSC is able to capture the surface at resolution up to 10 m.px^{-1} with field of view 11.9°, covering a 52.2 km wide strip of surface at height 250 km (which is the periapsis of MEX). The camera consists of 9 CCD sensors allowing it to acquire triple stereo images in 4 colors and 5 phase angles. What is a very useful property of these images, is that they are taken nearly simultaneously and thus having the same illumination and other observational conditions (which further helps in photogrammetric processing of the images).

HRSC also contains a super-high-resolution camera called SRC (*Super-Resolution Channel*) aimed at targeted observations of particular surface details. With image resolution 2.3 m.px^{-1} and field of view 0.54° it provides a detailed view of a

[1]A camera that scans the image by rows perpendicular to the flight direction. See `http://earthobservatory.nasa.gov/Features/EO1/eo1_2.php` for more details.

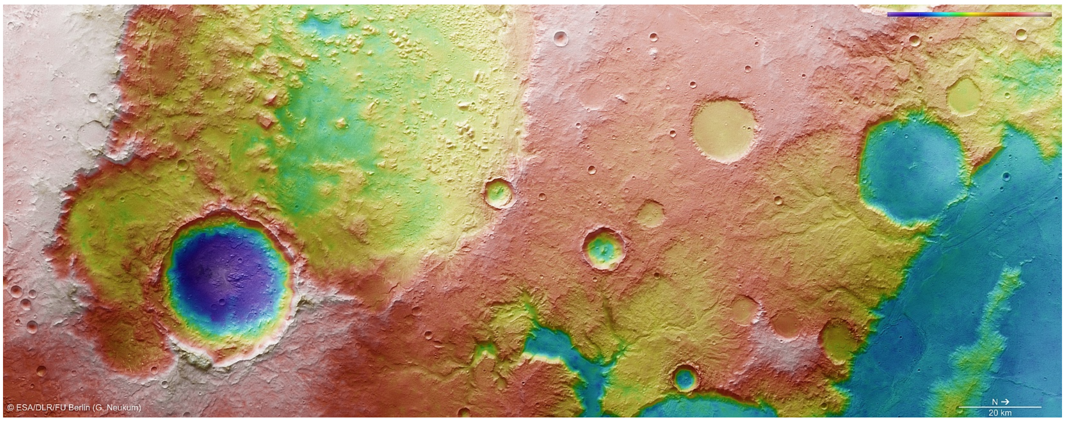

Figure 1.2: Example image taken by HRSC. Credit: ESA/DLR/FU Berlin (G. Neukum) [27]

2.3x2.35 km large surface. Its main purpose is to take details of places of interest, eg. future landing sites for other landing modules.

Up to November 2011 HRSC had covered about 88 % of the martian surface [16, pp. 72–73] and still continues to gather new data. The scientific results of HRSC are for example better exploration of fluviatile valleys [24], dicovery of numerous glacial landforms, investigating lava flows, dicovery of “dust devils” (fast moving dust storms) or providing data to derive a detailed topographic model of more than 20 % of Phobos [21, pp. 945–949].

1.1.2 OMEGA (*Observatoire pour la Minéralogie, l'Eau, les Glaces et l'Activité*)

OMEGA is a medium- and high-resolution spectrometer operating in visible and near-IR spectra (0.38–5.1 µm wavelength). Its medium-resolution operating mode (from heights of 1,500 to 4,000 km) can measure with the resolution 2–5 km targeting at global surface coverage, while the high-resolution mode (from the close vicinity of periapsis) brings resolution 350 m or better, but will cover only a small fraction of the surface.

As stated in [30, pp. 38–39], the main goals are to study the evolution of Mars, to detect minerals hidden to lower resolutions, to map mineralogical boundaries between geological units, to reveal gradients in hydration minerals related to fossil water flows and to monitor features associated with wind transportation. In particular, it is intended to find carbonates (not found on martian surface until the launch of MEX) and water ice. It is also able to measure atmospheric pressure, CO and H_2O column densities and surface temperature.

Recent contributions of the OMEGA payload are e.g. confirmation of liquid water on the surface when the planet was young [22], discovery of infrared and ultraviolet glows in the atmosphere [4], proving that Mars had a hot and wet period [7] (implying there were lots of greenhouse gases and a strong magnetic field, too [18, p. 90]), analyzing the south polar cap and finding out it is formed mainly of water ice [9], observation of CO_2 ice clouds [26] or finding ferric oxides near the equator [25].

1.1.3 MARSIS (*Mars Advanced Radar for Subsurface and Ionosphere Sounding*)

MARSIS is a long-wavelength radar using coherent wide-band pulses for sounding of the surface, subsurface and ionospehere of Mars. For these purposes it uses a 40 m dipole antenna (for both transmitting and receiving) and a shorter 7 m monopole antenna (only for receiving). Due to the used sounding frequencies ranging from 100 kHz to 5.5 MHz it is able to reach the depth about 5–8 km under the surface.

The primary goal of MARSIS is to detect liquid and solid water in the upper crust of Mars. There are also other objectives: subsurface geologic probing (to make a 3D characterization of the subsurface structures), surface characterization (to measure surface roughness, reflectance to radar signals and to estimate topography) and ionosphere sounding (to measure interaction between solar wind and the ionospehere) [30, p. 51].

To name some results of the MARSIS instrument, we can mention revealing the layered subsurface structure of both polar caps (strongly suggesting there were oceans in distant history at these places) [18, pp. 98–102] along with estimating the volume of subsurface water ice in the polar cap [29], discovery of *Medusae Fossae Formations* (the youngest surface deposits) [18, pp. 102–105] or mapping the ionosphere and verifying the ionospheric density models [18, pp. 105-110].

One surprising and unexpected utilization of the MARSIS instrument is given by the electron cyclotron echoes found in ionograms (see section 1.3.5). It was found that they often correspond to the strength of the magnetic field, effectively allowing to measure that field and compare it to its model. Another type of echoes, the oblique ionospheric echoes (see section 1.3.3) were identified to correspond to the crustal magnetic field. Both these contributions were made by [19].

1.1.4 PFS (*Planetary Fourier Spectrometer*)

PFS is IR-spectrometer (based on double-pendulum interferometer) operating in the range 1.2–42 μm divided into two channels – the *Short Wavelength* (SW) channel (1.2–5 μm) and the *Long Wavelength* (LW) channel (5–42 μm). Its spatial resolution is 10 km for SW and 20 km for LW (from altitude 300 km). PFS uses an onboard *Fast Fourier Transform* circuit to select only the data scientists are interested in.

The objectives of this device are atmospheric studies like atmospheric composition (as it can detect eg. H_2O, CO and CO_2 spectra), solid-phase surface components detection and atmospheric dust measurements. PFS also captures the vertical temperature–pressure profiles and dust and ice opacity [30, pp. 115–116].

The contributions made using PFS so far are for example measuring the atmospheric temperature (finding out that there is a rather complicated situation around the peak of Olympus Mons), measuring the surface temperature, counting the atmospheric dust content, observing temperature inversion effects, detecting methane in the atmosphere (which could imply either organic life or volcanic activity, which are both unexpected phenomena), proving that the south polar cap is made mainly from CO_2 ice, or capturing the solar spectrum from the surroundings of Mars (which cannot be done from Earth) [30, pp. 122–135].

1.1.5 SPICAM (*SPectroscopy for the Investigation of the Characteristics of the Atmosphere of Mars*)

The SPICAM instrument is made of two spectrometers, one operating in the UV spectrum (118–320 nm) and the other in the near-IR (1.0–1.7 μm).

Many tasks have been assigned to SPICAM, the major of them being investigating ozone, H_2O and aerosols vertical profiles in the atmosphere. These should help constructing meteorological and dynamical atmospheric models, understanding the water vapour atmospheric cycles, characterize processes of water escape from the atmosphere, investigating the interactions between surface and atmosphere and revealing impact of aerosols on martian climate [30, pp. 97–100].

One of the latest surprises brought by SPICAM is martian atmosphere is supersaturated with water vapour which further prepares conditions for water escape from the atmosphere [23]. Another unexpected result are nocturnal aurorae observed in the upper atmosphere, along with the (expected) NO recombination nightglow [5]. Other results involve retrieving global spatial and temporal climatology of ozone [28], south polar cap observations [18, pp. 158–159], studies of UV dayglow [18, pp. 160–162], constructing the aerosol vertical profiles [18, pp. 175–180] or observation of CO_2 clouds on the nightside [18, p. 178].

1.1.6 ASPERA–3 (*Analyser of Space Plasmas and EneRgetic Atoms*)

ASPERA–3 is an instrument designed to study the interaction between solar wind and martian atmosphere. It comprises of four separate detectors. The first one is *Neutral Particle Imager* (NPI) measuring the *energetic neutral atom* (ENA) flux with high angular resolution. Another one neutral atoms sensor, the *Neutral Particle Detector* (NPD), measures the neutral atom flux resolving energy and mass of the atoms. The other two instruments are aimed at electrically charged particles. The *Electron Spectrometer* (ELS) is a top-hat electrostatic analyzer, while the *Ion Mass Analyzer* (IMA) is an ion mass composition analyzer working with H^+, He^{2+}, He^+ and O^+ ions [30, p. 122].

ASPERA–3 should focus on measuring ENAs in order to investigate the interaction between solar wind and martian atmosphere, to characterize the impact of plasma processes on atmospheric evolution and to obtain plasma and neutral gas distribution near Mars. It should also measure electrons and ions to complement ENA measurements, to study the dynamics and structure of plasma and to provide solar wind parameters [30, p. 122].

To present some results of ASPERA–3 we can mention discovering that the solar wind penetrates much deeper in martian atmosphere than was believed, being one of the atmospheric ions escape mechanisms [2], detection of ENA jets caused by solar wind [18, pp. 208–209], observing the ENA flux during Mars eclipse which laid foundation of a new method to measure planetary exosphere [18, p. 209] or proving there is a yet unidentified source of interplanetary ENAs [18, pp. 209–212].

1.1.7 MaRS (*Mars Express Orbiter Radio Science*)

Opposite to the already described devices, the MaRS experiment doesn't have a dedicated physical device like a sensor or transmitter. Instead, it utilizes the communication antennas to perform radio occultation experiments. It can use either the parabolic 1.6 m diameter *High Gain Antenna* or the smaller *Low Gain Antennas*. The second part of the occultation experiments (namely the receivers) cannot be carried on board MEX, because they need to be on the opposite side of Mars than MEX is. Thus, the receivers are placed on Earth (Kourou, French Guayana; Darmstadt, Germany; Perth, Australia; plus 3 NASA's *Deep Space Network* telescopes in Goldstone, USA; Madrid, Spain and Canberra, Australia). The experiment uses two frequency bands – the S-band at 2.1 GHz and the X-band at 7.1 GHz [30, pp. 153–154].

MaRS is intended to sound the neutral atmosphere to derive vertical density, pressure and temperature profiles, to sound the ionosphere as well (in order to get electron density profiles), to determine the dielectric properties of the surface, to detect gravity anomalies and to sound the solar corona at extra occasions [30, p. 141].

MaRS contributed towards improving existing atmospheric *global circulation models* [18, p. 227], towards the discovery of so called "meteor layer" of atmosphere containing ionized metallic atoms brought into the atmosphere by meteoric impacts [18, p. 230] and towards refining the crustal structure [18, p. 234].

1.1.8 Beagle 2

Beagle 2 is the lander module MEX was equipped with. It detached from the spacecraft on 19 December 2003 (6 days before MEX orbit entry) and its touchdown was planned to 25 December 2003. However, it hasn't transmitted any signal after the martian atmosphere entry. As of February 2004 it was declared lost. No particular reason came out on inquiry into its fault [6].

To accomplish its main goal (searching for existing or former life, or at least for conditions allowing development of life in the past) it was equipped with several scientific tools. To begin with, the *Gas Analysis Package* is a mass spectrometer used for examining the surrounding atmospheric gases as well as rock and soil samples (heated in ovens in order to vaporize). The *X-Ray Spectrometer* studies the composition of rock and soil samples using X-Ray fluorescence spectrometry being able to detect metals like Fe, Mg, Al, Ti and others. Another spectrometer, the *Mössbauer Spectrometer* is able to analyze materials containing iron. Its *Stereo Camera System* was intended to acquire stereoscopic images of the landing site in various spectral ranges. One of the largest contributions to Beagle's main goal should have been brought by the *Microscopic Imager* (by searching for microscopic fossils). As a support for all the mentioned systems, the *Planetary Underground Tool* handles soil samples acquisition using a 1.5 m long drill. There is also a grinder available for removing unwanted material from the samples or the surrounding surface. There are also several sensors attached to Beagle 2 - the *oxidant sensor* monitoring the oxidizing effects of martian atmosphere, the *UV sensor* capturing the UVA and UVB spectral ranges (which are lethal for organisms), the *wind sensor* recording the speed and direction of wind, the *air pressure sensor* with resolution 0.003 hPa, the *air temperature sensor* with accuracy about 0.01 K and finally the *dust impact monitor* measuring the magnitude and impact rate of dust particles [30, pp. 165–191].

1.2 The MARSIS experiment

In this section we will discuss the individual parts of the MARSIS experiment. We are going to briefly describe the physical background of the experiments as well as the technical solution of the measurement mechanisms.

Figure 1.3: Visualization of the Beagle 2 lander on martian surface. Credit: Beagle 2 [3]

1.2.1 Subsurface sounding

The subsurface sounding attempts to detect the borders of the *cryosphere*, which is the crust layer in which the temperature remains constantly under the water-freezing point. Such borders can be identified owing to different dielectric properties of liquid water and ice or ice and atmospheric gases. The deeper border can be a water–ice interface because the cryosphere ends where the internal planetary heat flow raises the temperature above the water-melting point (so if there is a liquid water reservoir under the cryosphere, it can be detected). This interface is expected to be at 0–5,000 m depth. On the other hand, the higher border can be formed by the desiccated megaregolith (martian soil) where the desiccation is caused by subsurface ice sublimation (estimated to be at depths between 0 and 1,000 m) [30, pp. 52–53].

As described in part 1.1.3, MARSIS can utilize a 40 m long dipole antenna as well as a 7 m monopole one. Only the dipole antenna is used for signal transmission (generating up to 10 W strong signal), and both antennas for signal receipt. It can sound using one of the four subsurface frequency bands centered at 1.8, 3, 4 and 5 MHz, every one having its bandwidth of 1 MHz. When MEX operates on the dayside of Mars, the ionosphere doesn't allow to use lower frequency bands for sounding (see section 1.2.3), so only the last two bands can be used. On the nightside, all four bands get through the ionosphere and allow to sound deeper subsurface. However, due to the limitations given by the MEX spacecraft, only echoes from depths up to 5–8 km can be detected [30, p. 57].

The subsurface sounder mode is based on the fact that the radar waves reflect not only on the surface, but also on subsurface dielectric discontinuities. In addition, the velocity of the waves decreases proportionally to the material loss tangent, the wavelength and the depth – which facilitates computing the depth of subsurface interfaces [30, p. 56].

1.2.2 Surface sounding

It arises from the previous paragraphs that the surface sounding mode is a "subset" of the subsurface sounding mode, taking only the "topmost" echoes into account. Therefore, no additional operation modes are present for just the surface sounding.

The surface sounding is used to create a topography of the surface with lateral resolution 5–9 km. This topography further serves for improving the accuracy of statistical topography models which describe the surface in the means of a random distribution of heights [30, p. 54].

1.2.3 Ionospheric sounding

The basic reason for studying the ionosphere is that it stops propagation of electromagnetic waves with frequencies below the local *electron plasma frequency* $f_p = 8980\sqrt{N_e}$ Hz, where N_e is the local electron density in cm^{-3}. All vertical waves with frequencies below the maximum electron plasma frequency, $f_p(\max)$, are reflected back at a place with the same frequency as the waves have. This maximum is usually located at the heights 125–150 km and amounts up to 4 MHz on the dayside and 800 kHz on the nightside [30, pp. 55–56].

MARSIS uses two methods – a passive and an active one. The passive method measures thermal emission at the local electron plasma frequency. The active method – the one of our interest – sounds the ionosphere with the radar in 160 frequency steps ranging from 100 kHZ to 5.4 MHz. Every pulse has a duration of 91.4 ms. With such a sampling it is possible to construct vertical profiles of the electron plasma frequency (and also electron density). Besides the normal ionospheric sounding mode, MARSIS also provides a special interleaved mode switching periodically between the subsurface sounding and ionosphere sounding modes. This yields a method to remove the ionospheric effects from the subsurface sounding results [30, p. 58].

Adding to the ionospheric and surface echoes, there are three more (unexpected [19, p. 1930], but useful) signal patterns detectable using the ionospheric sounding. Namely, oblique ionospheric echoes, electron plasma oscillation har-

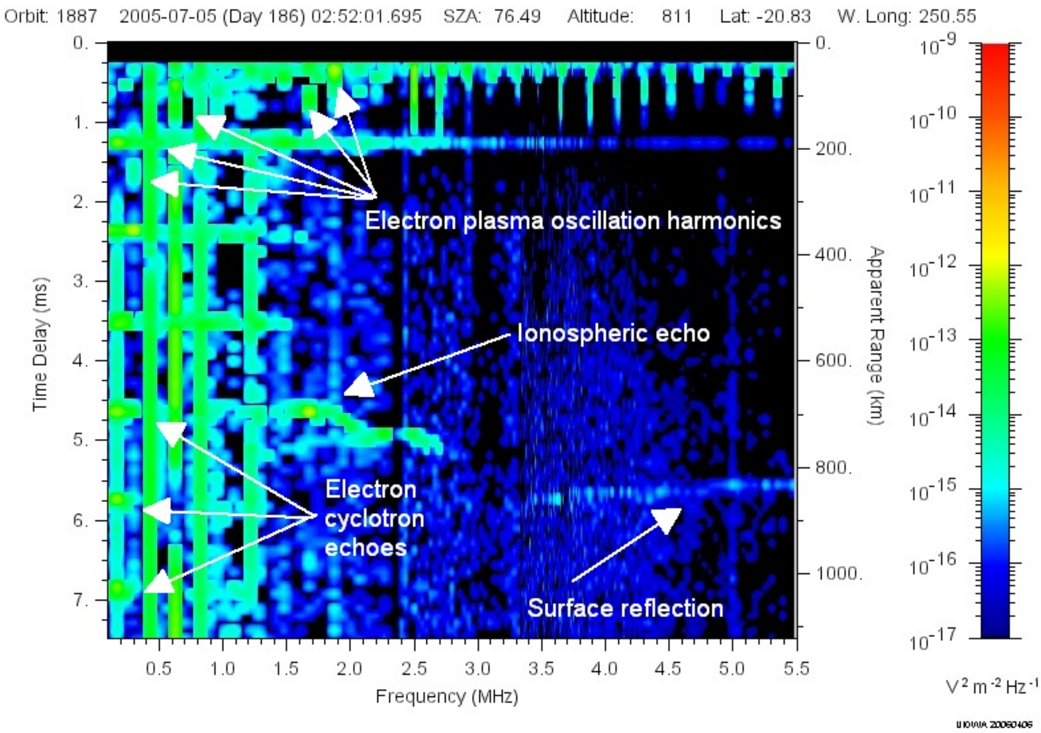

Figure 1.4: Example of a ionogram showing most of the detectable features like ionospheric echo, surface reflection, electron cyclotron echoes and electron plasma oscillation harmonics. No oblique ionospheric echo is present. The vertical axis shows delay time in ms, the horizontal axis stands for frequency in MHz and color codes the spectral density of the received electric field in $V^2m^{-2}Hz^{-1}$. Based on real data obtained from [20].

monics and electron cyclotron echoes. We will describe all of them in the following sections after presenting the concept of ionograms.

1.3 Ionograms

Ionograms are the basic visualization of the ionospheric sounding data. Akalin [1] defines ionograms in the following precise way:

> Ionograms are produced by transmitting a short pulse at a fixed frequency, f, and measuring the received intensity at 80 consecutive values of the time delay, Δt, spaced 91.4 µs apart. The frequency is then incremented and the process is repeated. For each of 160 frequencies, quasi-logarithmically spaced between 0.1 and 5.5 MHz, there are 80 delay time bins, spaced 91.4 µs apart, beginning 162.5 µs after the end of the sounding pulse. Ionograms represent received intensity as a function of time delay and frequency. As shown by the ionogram in Fig. 1.4, time delay is displayed in milliseconds along the vertical

axis, frequency is displayed in megahertz along the horizontal axis, and the color bar represents the received electric field spectral density in $V^2m^{-2}Hz^{-1}$.

Several more or less continuous patterns can be found in the example ionogram. Some of them form repetitious patterns. It can be also seen that the data are very noisy. The example ionogram is rather rare, because often just one or two such patterns occur in a single ionogram. There are also ionograms consisting entirely of noise. The subsequent sections will discuss all the patterns and their physical meaning.

1.3.1 Ionospheric echo

As seen in Fig. 1.4, the ionospheric echo is a horizontally oriented non-straight line. It usually appears in the lower half of the ionogram (delay times about 4 to 5 ms). Its left end is located where the local f_p frequency starts to be higher than the sounding frequency, which is most often somewhere below 1 MHz. Its right end should be placed at $f_p(\max)$ frequency, where all higher-frequency waves pass to the surface [19, p. 1929].

There is often a sharp cusp at the right end of the echo. "The cusp occurs because the propagation speed of the wave packet (i.e., the group velocity) is very small over an increasingly long path length as the wave frequency approaches $f_p(\max)$" [19, p. 1929]. On the other hand, the echo often doesn't extend up to $f_p(\max)$ [19, p. 1930].

As we have mentioned earlier, it is possible to read out the local electron plasma frequency from the echo, thus obtaining the electron density vertical profile. In order to extract the profile, it is needed to identify the curve fitting the echo. Automatic identification of such curve is one of the goals of this work. Especially correct estimation of the right end would be helpful if the cusp is present.

1.3.2 Surface echo

Similar to the ionospheric echo is the surface echo. It is placed lower than the ionospheric echo (because the ionosphere is closer to the sounder than surface is). Its left end is at the same frequency where the ionospheric echo's right end should be, i.e. at the $f_p(\max)$ frequency. It should extend up to the right edge of the ionogram (since all frequencies higher than $f_p(\max)$ penetrate the ionosphere) [19, p. 1929].

The same (but mirrored) cusp as in ionospheric echo should be present at the left end of the surface echo, caused by the same effect.

It is common that there is no surface echo in the ionogram. It can have several reasons. One of them is that the surface absorption of the radar waves increases

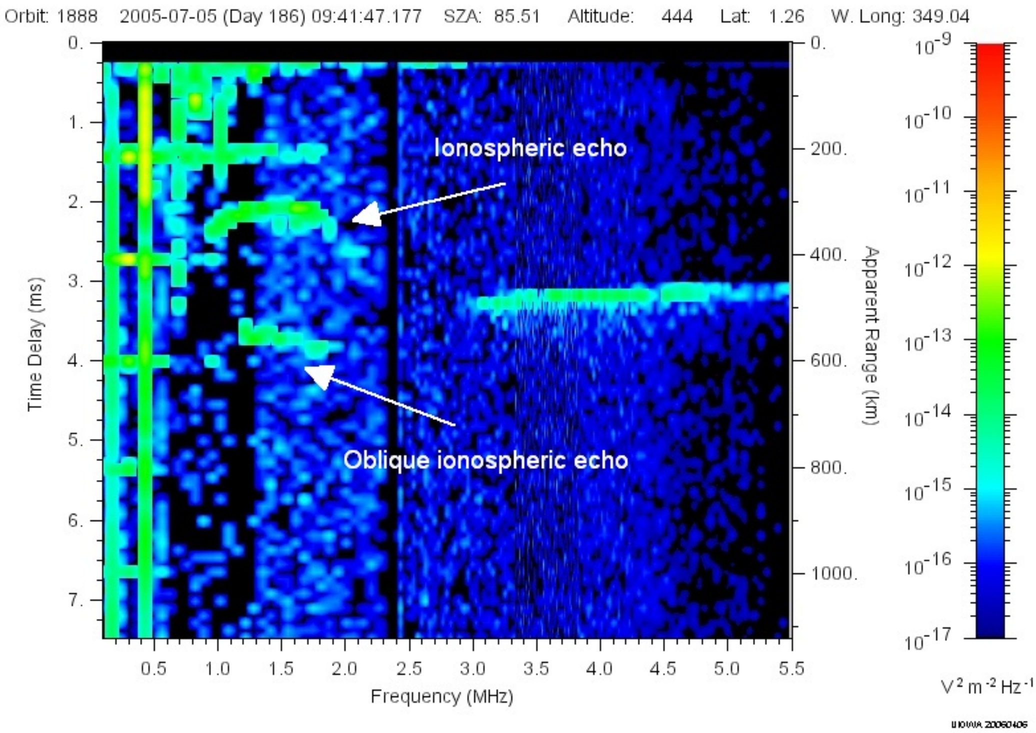

Figure 1.5: A ionogram containing oblique ionospheric echo. It is worth notice that the echo appears to origin under the surface level (because of the delay time higher than the delay time to surface). Based on real data obtained from [20].

with decreasing solar zenith angle (at angles lower than 40° the surface echoes are rare). Another way to stop the waves from returning to the sounder could be charged particles from solar flares ionizing the lower levels of ionosphere [19, p. 1930].

From surface echoes it is easy to read the apparent height over surface (omitting the cusp area), hence to create topographical maps and models. However, due to the frequent problems with absorption, it is not a good primary means of creating complete topographical maps since lots of the data are missing.

1.3.3 Oblique ionospheric echo

The first of unexpected features emergent in ionograms are oblique ionospheric echoes. An example of such echo is displayed in Fig. 1.5. It is an echo of similar shape and horizontal boundaries as the ionospheric echo, but located a few ms lower in the ionogram. Often even lower than the surface echo – but the radar waves don't even reach the surface at the frequencies of the ionospheric echo.

An explanation of this effect is given in [19, pp. 1931–1933]. At locations with strong crustal magnetic field, this field forms bulges in the ionosphere. Such bulges, if lying aside the MEX track, reflect the waves from the sounder under

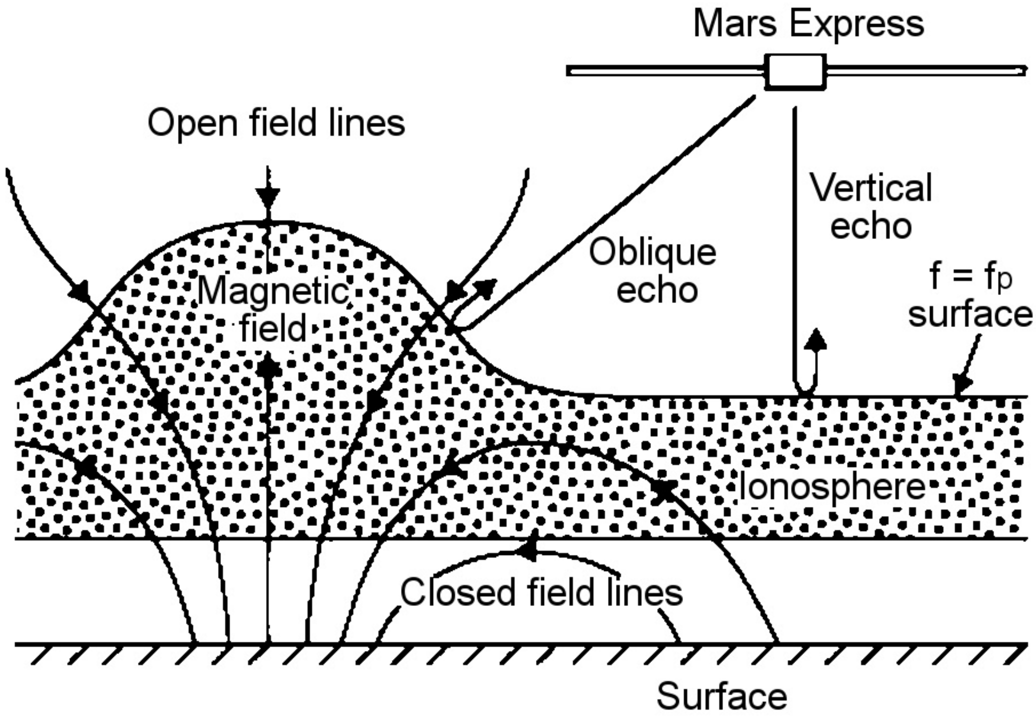

Figure 1.6: A ionospheric bulge created by strong crustal magnetic field can produce oblique ionospheric echoes. [19]

such angle that the antenna records the reflections. However, since the track of these waves isn't vertical, they may travel longer distances than to the surface before they return. An illustration of this effect is provided in Fig. 1.6.

To detect oblique echoes in ionograms could be of some use, because they point to places with ionosphere bulges and strong crustal fields. However, deriving the shapes of the bulges or the crustal fields would be very complicated [19, p. 1932]. Therefore, we won't try to detect them in the task-specific algorithms devised in this thesis.

1.3.4 Electron plasma oscillation harmonics

Another surprise are repetitious straight vertical lines in ionograms, electron plasma oscillation harmonics (called also Langmuir waves [10, p. 2]). As can be seen in Fig. 1.4, they appear near the top left corner of ionograms. They always start at the top of the image and continue towards the bottom; they may disappear on any time delay. Although they are mainly located in the left part of ionograms, occasionally the may repeat up to the right edge. More than 10 repetitions are, however, rare [10, p. 4].

It is stated in [19, p. 1929] that these echoes "are at harmonics of the local electron plasma frequency and are caused by the excitation of electron plasma oscillations, [. . .]. Even if the fundamental of the plasma frequency is not observed directly [. . .], the plasma frequency can still be determined from the spacing of the harmonics." The reason why not only the base frequency is present, but also its harmonics, is described in [10, p. 2]: "Since the electron plasma oscillations are usually very intense, [...] the received waveforms are often severely clipped. The resulting distortion then introduces harmonics at multiples of the basic oscillation frequency."

As all features detected by the ionospheric sounders, also plasma oscillation harmonics may not be present in a ionogram. There are three main reasons for it: when the local electron density is less than $10\,\mathrm{cm}^{-3}$, when the plasma flow velocity is more than 160 km/h or when the temperature is greater than 8,521 n_e °K (n_e stands for electron density in cm^{-3}; this happens in solar wind) [10, p. 4].

Although the base oscillation frequency is occasionally captured in ionograms (when higher than 100 kHz, the sounder's lowest frequency), it is apparently more precise to derive the frequency from the harmonics spacing (using multiple fit). That is what we will focus on in later chapters.

As a benefit, this method allows to measure the electron density in heights up to 1,300 km which corresponds to very low densities. Such low densities couldn't be detected by the radar sounder.

1.3.5 Electron cyclotron echoes

The last unanticipated phenomenon appearing in ionograms are the electron cyclotron echoes. These are regularly-repeating straight horizontal lines in ionograms. They always start from the lowest sounding frequency (the left edge) and extend to frequencies up to 2 MHz [1, p. 3]. It can be observed in Fig. 1.4 that the repetition can appear at the whole vertical range.

Comparing with the magnetic field model of Mars, [19] determined that the repetition frequency of these echoes corresponds to local electron cyclotron frequency f_c. That frequency can be expressed as $f_c = 28\ B$ Hz, B being the magnetic field strength in nT. Thus, knowing the repetition rate of the echoes, we are able to determine the strength of the magnetic field. That is a very important application, since MEX doesn't carry a magnetometer [19, p. 1930]. There is also a method to derive the vector component of the magnetic field under some conditions [1].

The origin of these echoes is described in [19, p. 1930]: "We believe that these echoes are caused by electrons accelerated by the strong electric fields near the antenna during each cycle of the transmitter waveform. The cyclotron motion of the electrons in the local magnetic field then causes these electrons to periodically return to the vicinity of the antenna, where they induce a signal on the antenna."

Some constraints, of course, apply to the presence of cyclotron echoes in ionograms. Firstly, the magnetic field strength must be uniform on an area larger than the cyclotron radius (which is about 1 km). According to [19, p. 1930] this is easily satisfied. Further, the sounder's minimum and maximum time delay resolution constrains the detectable field strengths. The minimum resolution of 182.2 μs corresponds to field strength of 195 nT, while the maximum delay of 7.5 ms corresponds to field strength of about 5 nT. However, in practice the reasonable range for confident measurements is about 12 – 160 nT [1, p. 3].

Similarly to the plasma oscillation harmonics, we are interested in the period of repetition of these echoes. If we can compute it, we are able to compute the strength of the magnetic field and, in some cases, also its direction. We will also focus on detection of this period in our survey.

2. Title of the second chapter

2.1 Title of the first subchapter of the second chapter

2.2 Title of the second subchapter of the second chapter

Conclusion

Bibliography

[1] AKALIN, F. et al. Dayside induced magnetic field in the ionosphere of Mars. *Icarus*. March 2010, 206, 1, pages 104–111. ISSN 00191035. doi: 10.1016/j.icarus.2009.03.021. Available from: `http://linkinghub.elsevier.com/retrieve/pii/S0019103509001316`.

[2] BARABASH, S. et al. Martian atmospheric erosion rates. *Science (New York, N.Y.)*. January 2007, 315, 5811, pages 501–3. ISSN 1095-9203. doi: 10.1126/science.1134358. Available from: `http://www.ncbi.nlm.nih.gov/pubmed/17255508`.

[3] BEAGLE_2. *Beagle 2 lander*. In *Space In Images* [online], 2002. [Accessed 03/24/2013]. Available from: `http://spaceinimages.esa.int/Images/2001/11/Beagle_2_lander`.

[4] BERTAUX, J. L. et al. First detection of O 2 1.27 μ m nightglow emission at Mars with OMEGA/MEX and comparison with general circulation model predictions. *Journal of Geophysical Research*. March 2012, 117, pages E00J04. ISSN 0148-0227. doi: 10.1029/2011JE003890. Available from: `http://www.agu.org/pubs/crossref/2012/2011JE003890.shtml`.

[5] BERTAUX, J.-L. et al. Nightglow in the upper atmosphere of Mars and implications for atmospheric transport. *Science (New York, N.Y.)*. January 2005, 307, 5709, pages 566–9. ISSN 1095-9203. doi: 10.1126/science.1106957. Available from: `http://www.ncbi.nlm.nih.gov/pubmed/15681381`.

[6] BONACINA, F. *Lessons Learnt From Beagle 2 And Plans To Implement Recommendations From The Commision Of Inquiry*. In *Ireland / ESA in your country* [online], 2004. [Accessed 03/24/2013]. Available from: `http://www.esa.int/ESA_in_your_country/Ireland/Lessons_learnt_from_Beagle_2_and_plans_to_implement_recommendations_from_the_Commission_of_Inquiry`.

[7] CHEVRIER, V., POULET, F., BIBRING, J.-P. Early geochemical environment of Mars as determined from thermodynamics of phyllosilicates. *Nature*. July 2007, 448, 7149, pages 60–3. ISSN 1476-4687. doi: 10.1038/nature05961. Available from: `http://www.ncbi.nlm.nih.gov/pubmed/17611538`.

[8] CLARK, S. *Mars Express back in business at the red planet*. In *Spaceflight Now* [online], 2012. [Accessed 03/20/2013]. Available from: `http://www.spaceflightnow.com/news/n1202/15marsexpress/`.

[9] DOUTé, S. et al. South Pole of Mars: Nature and composition of the icy terrains from Mars Express OMEGA observations. *Planetary and Space Science*. January 2007, 55, 1-2, pages 113–133. ISSN 00320633. doi: 10.1016/j.pss.2006.05.035. Available from: `http://linkinghub.elsevier.com/retrieve/pii/S0032063306001243`.

[10] DURU, F. et al. Electron densities in the upper ionosphere of Mars from the excitation of electron plasma oscillations. *Journal of Geophysical Research*. 2008, 113, A7, pages A07302. ISSN 0148-0227. doi: 10.1029/2008JA013073. Available from: `http://www.agu.org/pubs/crossref/2008/2008JA013073.shtml`.

[11] ESA. MARS EXPRESS MASTER SCIENCE PLAN Part I - Introduction. Technical Report 1, 2004. Available from: `http://www.rssd.esa.int/SB/MARSEXPRESS/docs/MSPDOC/MSPOverviewDocumentation-PartI.pdf`.

[12] ESA. *Mars Express Radar Deployment Postponed*. In *ESA Science & Technology* [online], 2004. [Accessed 03/20/2013]. Available from: `http://sci.esa.int/science-e/www/object/index.cfm?fobjectid=35021`.

[13] ESA. *Mars Express 2nd Boom Deployed*. In *ESA Science & Technology* [online], 2005. [Accessed 03/20/2013]. Available from: `http://sci.esa.int/science-e/www/object/index.cfm?fobjectid=37608`.

[14] ESA. *Mars Express and the mystery of Phobos*. In *ESA Kids Liftoff* [online], 2010. [Accessed 20. 3. 2013]. Available from: `http://www.esa.int/esaKIDSen/SEM8534KV5G_Liftoff_1.html`.

[15] ESA. *Mars Express steadily returns to routine operation*. In *ESA Our Activities* [online], 2011. [Accessed 03/20/2013]. Available from: `http://www.esa.int/Our_Activities/Operations/Mars_Express_steadily_returns_to_routine_operation`.

[16] ESA. Programmes in Progress. *Bulletin Space for Europe issue 148*. 2011, pages 72–73. Available from: `http://esamultimedia.esa.int/multimedia/publications/ESA-Bulletin-148/pageflip.html`.

[17] ESA. *Fact Sheet*. In *ESA Science & Technology* [online], 2013. [Accessed 03/20/2013]. Available from: `http://sci.esa.int/science-e/www/object/index.cfm?fobjectid=47364`.

[18] FLETCHER, K., WITASSE, O. *MARS EXPRESS: The Scientific Investigations*. Noordwijk, Netherlands : ESA Communication Production Office ESTEC, PO Box 299, 2200 AG Noordwijk, Netherlands,

2009. Available from: http://sci.esa.int/science-e/www/object/index.cfm?fobjectid=47218. ISBN 978-92-9221-975-8.

[19] GURNETT, D. a. et al. Radar soundings of the ionosphere of Mars. *Science (New York, N.Y.)*. December 2005, 310, 5756, pages 1929–33. ISSN 1095-9203. doi: 10.1126/science.1121868. Available from: http://www.ncbi.nlm.nih.gov/pubmed/16319123.

[20] GURNETT, D. A. *Mars Epxress MARSIS: Restricted Access*. In *University of Iowa* [online], 2005. [Accessed 03/26/2013]. Available from: ftp://www-pw.physics.uiowa.edu/plasma-wave/marsx/restricted/super/DATA/ACTIVE_IONOSPHERIC_SOUNDER/.

[21] JAUMANN, R. et al. The high-resolution stereo camera (HRSC) experiment on Mars Express: Instrument aspects and experiment conduct from interplanetary cruise through the nominal mission. *Planetary and Space Science*. May 2007, 55, 7-8, pages 928–952. ISSN 00320633. doi: 10.1016/j.pss.2006.12.003. Available from: http://linkinghub.elsevier.com/retrieve/pii/S0032063306003448.

[22] LOIZEAU, D. et al. Characterization of hydrated silicate-bearing outcrops in Tyrrhena Terra, Mars: Implications to the alteration history of Mars. *Icarus*. May 2012, 219, 1, pages 476–497. ISSN 00191035. doi: 10.1016/j.icarus.2012.03.017. Available from: http://linkinghub.elsevier.com/retrieve/pii/S0019103512001108.

[23] MALTAGLIATI, L. et al. Evidence of water vapor in excess of saturation in the atmosphere of Mars. *Science (New York, N.Y.)*. September 2011, 333, 6051, pages 1868–71. ISSN 1095-9203. doi: 10.1126/science.1207957. Available from: http://www.ncbi.nlm.nih.gov/pubmed/21960630.

[24] MANGOLD, N. et al. Geomorphic study of fluvial landforms on the northern Valles Marineris plateau, Mars. *Journal of Geophysical Research*. August 2008, 113, E8, pages E08009. ISSN 0148-0227. doi: 10.1029/2007JE002985. Available from: http://www.agu.org/pubs/crossref/2008/2007JE002985.shtml.

[25] MASSé, M. et al. Mineralogical composition, structure, morphology, and geological history of Aram Chaos crater fill on Mars derived from OMEGA Mars Express data. *Journal of Geophysical Research*. December 2008, 113, E12, pages E12006. ISSN 0148-0227. doi: 10.1029/2008JE003131. Available from: http://www.agu.org/pubs/crossref/2008/2008JE003131.shtml.

[26] MONTMESSIN, F. et al. Hyperspectral imaging of convective CO 2 ice clouds in the equatorial mesosphere of Mars. *Journal of Geophysical Research*. November 2007, 112, E11, pages E11S90. ISSN 0148-0227. doi: 10.1029/2007JE002944. Available from: `http://www.agu.org/pubs/crossref/2007/2007JE002944.shtml`.

[27] NEUKUM, G. *Amenthes Planum topography*. In *Space In Images* [online], 2013. [Accessed 03/21/2013]. Available from: `http://spaceinimages.esa.int/Images/2013/02/Amenthes_Planum_topography`.

[28] PERRIER, S. et al. Global distribution of total ozone on Mars from SPICAM/MEX UV measurements. *Journal of Geophysical Research*. 2006, 111, E9, pages E09S06. ISSN 0148-0227. doi: 10.1029/2006JE002681. Available from: `http://www.agu.org/pubs/crossref/2006/2006JE002681.shtml`.

[29] PHILLIPS, R. J. et al. Mars north polar deposits: stratigraphy, age, and geodynamical response. *Science (New York, N.Y.)*. May 2008, 320, 5880, pages 1182–5. ISSN 1095-9203. doi: 10.1126/science.1157546. Available from: `http://www.ncbi.nlm.nih.gov/pubmed/18483402`.

[30] WILSON, A. (Ed.). *Mars Express: the scientific payload*. Noordwijk, Netherlands : ESA Publications Division, 2004. Available from: `www.esa.int/esapub/sp/sp1240/sp1240web.pdf`. ISBN 92-9092-556-6.

List of Tables

List of Abbreviations

Attachments